



This is the accepted manuscript made available via CHORUS. The article has been published as:

# Phase Space Reconstruction from Accelerator Beam Measurements Using Neural Networks and Differentiable Simulations

R. Roussel, A. Edelen, C. Mayes, D. Ratner, J. P. Gonzalez-Aguilera, S. Kim, E. Wisniewski,  
and J. Power

Phys. Rev. Lett. **130**, 145001 — Published 5 April 2023

DOI: [10.1103/PhysRevLett.130.145001](https://doi.org/10.1103/PhysRevLett.130.145001)

# Phase Space Reconstruction from Accelerator Beam Measurements Using Neural Networks and Differentiable Simulations

R. Roussel,\* A. Edelen, C. Mayes, and D. Ratner  
*SLAC National Accelerator Laboratory, Menlo Park, CA 94025, USA*

J.P. Gonzalez-Aguilera  
*Department of Physics, University of Chicago, Chicago, Illinois 60637, USA*

S. Kim, E. Wisniewski, J. Power  
*Argonne National Laboratory, Argonne, Illinois 60439, USA*  
(Dated: January 24, 2023)

Characterizing the phase space distribution of particle beams in accelerators is a central part of accelerator understanding and performance optimization. However, conventional reconstruction-based techniques either use simplifying assumptions or require specialized diagnostics to infer high-dimensional ( $> 2D$ ) beam properties. In this Letter, we introduce a general-purpose algorithm that combines neural networks with differentiable particle tracking to efficiently reconstruct high-dimensional phase space distributions without using specialized beam diagnostics or beam manipulations. We demonstrate that our algorithm accurately reconstructs detailed 4D phase space distributions with corresponding confidence intervals in both simulation and experiment using a single focusing quadrupole and diagnostic screen. This technique allows for the measurement of multiple correlated phase spaces simultaneously, which will enable simplified 6D phase space distribution reconstructions in the future.

Increasingly precise control of the distribution of particles in position-momentum phase space is needed for emerging applications of accelerators [1]. This includes, for example, new experiments at free electron lasers [2–6] and novel acceleration schemes that promise higher-energy beams in compact spaces [7]. Numerous techniques have been developed for precision shaping of beam distributions [8]; however, the effectiveness of these techniques relies on accurate measurements of the 6D phase space distribution, which is a challenging task unto itself.

Tomographic measurement techniques are used in accelerators to determine the density distribution of beam particles in phase space  $\rho(x, p_x, y, p_y, z, p_z)$  from limited measurements [9–14]. The simplest form of this uses scalar metrics, such as second-order moments, to describe observations of the transverse beam distribution when projected onto a scintillating screen. [15–17]. This process however discards significant amounts of information about the beam distribution captured by high-resolution diagnostic screens and only predicts scalar quantities of the beam distribution. In contrast, methods using projections of the beam image, including filtered back-projection [12, 18], algebraic reconstruction [19–21], and maximum entropy tomography (MENT) [13, 22] produce more accurate reconstructions.

The MENT algorithm is particularly well-suited to reconstructing beams from limited and/or partial information sources about the beam distribution, as is the case in most experimental accelerator measurements. MENT solves for a phase space distribution that maximizes entropy (and, as a result, likelihood), subject to the constraint that the distribution accurately reproduces ex-

perimental measurements. While these techniques have been shown to effectively reconstruct 2D phase spaces from image projections using algebraic methods, application to higher-dimensional spaces requires independence assumptions between the phase spaces of principal coordinate axes  $(x, y, z)$ , complicated phase space rotation procedures [20, 23], or simultaneous measurement of multiple 2D sub-spaces with specialized diagnostic hardware [24].

Numerical optimization methods can also be used to infer beam distributions from experimental data. For example, arbitrary beam distributions can be parameterized by a set of principal components [25] whose relative weights can be optimized to produce a beam distribution that, when tracked through a simulation, reproduces experimental measurements. Alternatively, heuristics can be used to delete or generate particles in a distribution until particle tracking results match experiments [26, 27]. Unfortunately, these methods suffer from increasing computational cost when extending them to reconstructing high-dimensional phase space distributions, primarily due to the cost associated with optimizing the large number of free parameters needed to represent detailed beam characteristics in high-dimensional phase spaces.

In this Letter we describe a new method that provides detailed reconstructions of the beam phase space using simple and widely-available accelerator elements and diagnostics. To achieve this, we take advantage of recent developments in machine learning to introduce two new concepts (shown in Fig. 1): a method for parameterizing arbitrary beam distributions in 6D phase space, and a differentiable particle tracking simulation that allows

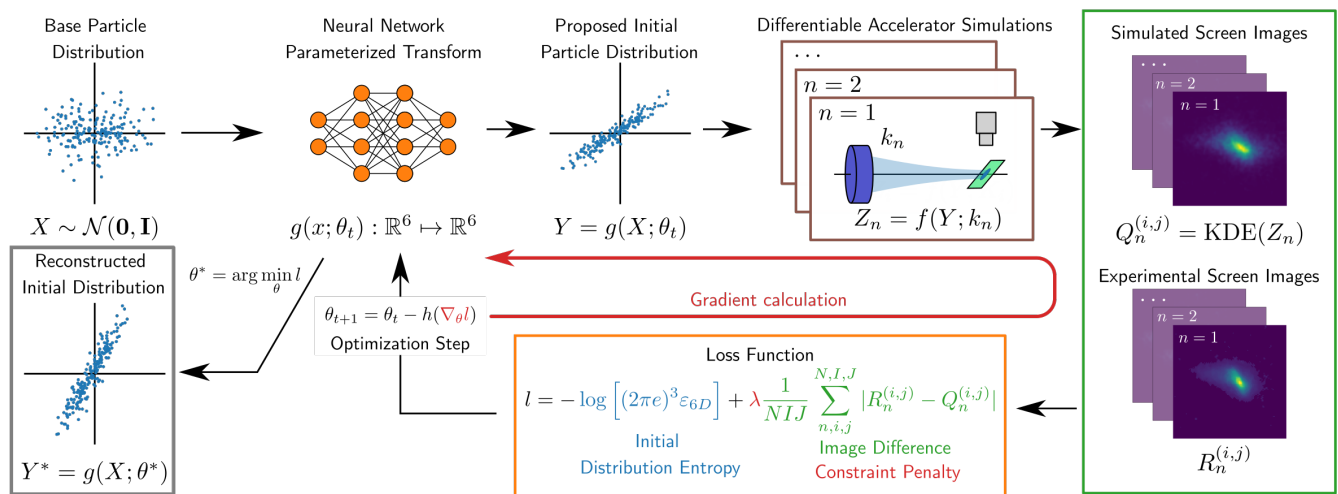


FIG. 1. Description of our approach for reconstructing phase space beam distributions. First, a 6D base distribution is transformed via neural network, parameterized by  $\theta_t$ , into a proposed initial distribution. This distribution is then transported through a differentiable accelerator simulation of the tomographic beamline. The quadrupole is scanned to produce a series of images on the screen, both in simulation and on the operating accelerator. The images produced both from the simulation  $Q_n^{(i,j)}$  and the accelerator  $R_n^{(i,j)}$  are then compared with a custom loss function, which attempts to maximize the entropy of the proposal distribution, constrained on accurately reproducing experimental measurements. This loss function is then used to update the neural network parameters  $\theta_t \rightarrow \theta_{t+1}$  via gradient descent. The neural network transformation that minimizes the loss function generates the beam distribution that has the highest likelihood of matching the real initial beam distribution.

74 us to learn the beam distribution from arbitrary down-  
 75 stream accelerator measurements. We examine how this  
 76 method extracts detailed 4-dimensional phase space dis-  
 77 tributions from measurements in simulation and exper-  
 78 iment, using a simple diagnostic beamline, containing a  
 79 single quadrupole, drift and diagnostic screen to image  
 80 the transverse  $(x, y)$  beam distribution. Finally, we dis-  
 81 cuss current limitations of this method as well as future  
 82 directions for the design of novel accelerator diagnostics  
 83 using this technique.

84 We first demonstrate our algorithm using a synthetic  
 85 example, where we attempt to determine the distribu-  
 86 tion of a 10-MeV beam given a predefined structure in  
 87 6D phase space. The propagation of a synthetic beam  
 88 distribution through a simple diagnostic beamline con-  
 89 taining a 10 cm long quadrupole followed by a 1.0 m drift  
 90 is simulated using a custom implementation of Bmad [28]  
 91 referred to here as Bmad-X. To illustrate the capabilities  
 92 of our technique, the synthetic beam contains multiple  
 93 higher order moments between each phase space coordi-  
 94 nates (see Supplemental Materials for details). To simu-  
 95 late an experimental measurement, we simulate partic-  
 96 les traveling through the diagnostic beamline while the  
 97 quadrupole strength  $k$  is scanned over  $N$  points. The  
 98 final transverse distribution of the beam is measured at  
 99 each quadrupole strength using a simulated  $200 \times 200$   
 100 pixel screen, with a pixel resolution of  $300 \mu\text{m}$  (image  
 101 data can be viewed in the Supplemental Materials). The  
 102 set of images, where the intensity of pixel  $(i, j)$  on the  $n$ 'th  
 103 image is represented by  $R_n^{(i,j)}$ , is then collected with the

104 corresponding quadrupole strengths to create the data  
 105 set, which is then split into training and testing subsets  
 106 by selecting every other sample as a test sample, result-  
 107 ing in 10 samples for each data subset.

108 The reconstruction algorithm begins with the gener-  
 109 ation of arbitrary initial beam distributions (referred to  
 110 here as proposal distributions) through the use of a neural  
 111 network transformation. A neural network, consisting of  
 112 only 2 fully-connected layers of 20 neurons each, is used  
 113 to transform samples drawn from a 6D normal distribu-  
 114 tion centered at the origin to macro-particle coordinates  
 115 in real 6D phase space (where positional coordinates are  
 116 given in meters and momentum coordinates are in radi-  
 117 ans for transverse momenta). As a result, the coordi-  
 118 nates of particles in the proposal distribution are fully param-  
 119 eterized by the neural network parameter set  $\theta_t$ .

120 Fitting neural network parameters to experimental  
 121 measurements is done by minimizing a loss function to  
 122 determine the most likely initial beam distribution, sub-  
 123 ject to the constraint that it reproduces experimental  
 124 measurements; this is similar to the MENT algorithm  
 125 [22]. The likelihood of an initial beam distribution in  
 126 phase space is maximized by maximizing the distribution  
 127 entropy, which is proportional to the log of the 6D beam  
 128 emittance  $\varepsilon_{6D}$  [29]. Thus, we specify a loss function that  
 129 minimizes the negative entropy of the proposal beam dis-  
 130 tribution, penalized by the degree to which the proposal  
 131 distribution reproduces measurements of the transverse  
 132 beam distribution at the screen location. To evaluate  
 133 the penalty for a given proposal distribution, we track

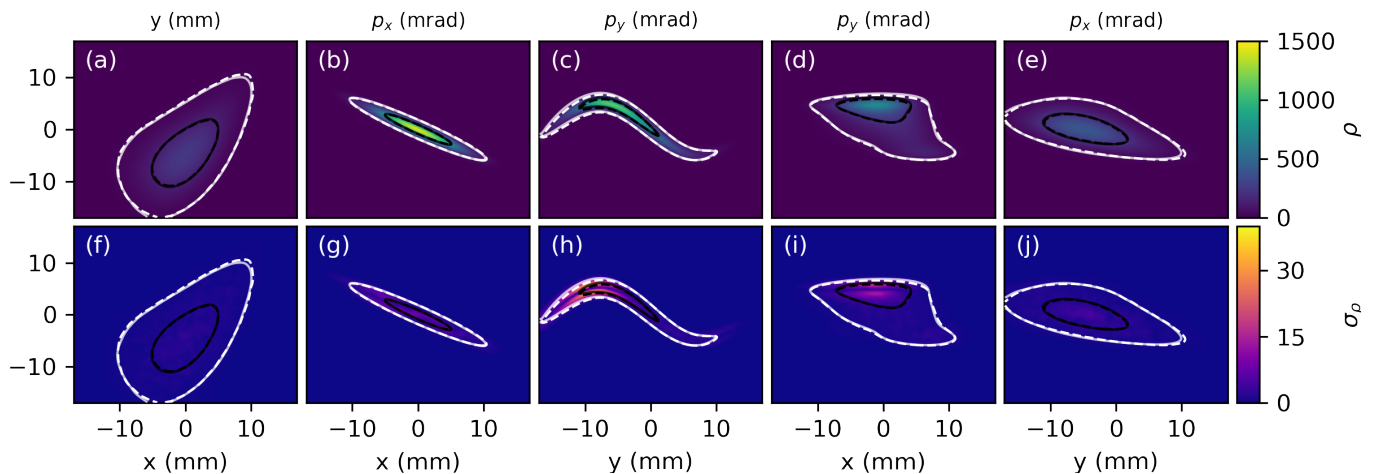


FIG. 2. Comparisons between the synthetic and reconstructed beam probability distributions using our method. (a-e) Plots of the mean predicted phase space density projections in 4D transverse phase space. Contours that denote the 50<sup>th</sup> (black) and 95<sup>th</sup> (white) percentiles of the synthetic ground truth (dashed) and reconstructed (solid) distributions. (f-j) Plots of the predicted phase space density uncertainty.

134 the proposal distribution through a batch of accelerator  
 135 simulations that mimic experimental conditions to gen-  
 136 erate a set of simulated images  $Q_n^{(i,j)}$  to compare with  
 137 experimental measurements. The total loss function is  
 138 given by

$$l = -\log \left[ (2\pi e)^3 \varepsilon_{6D} \right] + \lambda \frac{1}{NIJ} \sum_{n,i,j}^{N,I,J} |R_n^{(i,j)} - Q_n^{(i,j)}| \quad (1)$$

139 where  $\lambda$  scales the distribution loss penalty function rel-  
 140 ative to the entropy term and is chosen empirically based  
 141 on the resolution of the images.

142 However, the large ( $> 10^3$ ) number of free param-  
 143 eters contained in the neural network transformation used  
 144 to generate proposal distributions necessitates the use  
 145 of gradient-based optimization algorithms such as Adam  
 146 [30] to minimize the loss function. Thus, we need to  
 147 implement computation of the loss function such that it  
 148 supports backward differentiation [31] (referred to here  
 149 as *differentiable* computations), allowing us to cheaply  
 150 compute loss function derivatives with respect to ev-  
 151 ery neural network parameter. This requires that ev-  
 152 ery step involved in calculating the loss function is also  
 153 differentiable, including computing the beam emittance  
 154 and tracking particles through the accelerator. Unfortu-  
 155 nately, to the best of our knowledge, no particle tracking  
 156 codes currently support backwards differentiation. To  
 157 satisfy this requirement, we implement particle tracking  
 158 in Bmad-X using the machine learning library *PyTorch*  
 159 [32]. We estimate screen pixel intensities from a discrete  
 160 particle distribution with a differentiable implementation  
 161 of kernel density estimation [33].

162 Results from our reconstruction of the initial beam  
 163 phase space using synthetic images are shown in Fig. 2.  
 164 We characterize the uncertainty of our reconstruction us-

165 ing snapshot ensembling [34]. During model training,  
 166 we cycle the learning rate of gradient descent in a peri-  
 167 odic fashion which encourages the optimizer to explore  
 168 multiple possible solutions (if they exist). After several  
 169 of these cycles (known as a “burn-in” period), we save  
 170 model parameters at each minima of the learning rate  
 171 cycle, as shown in Fig. 3(a). We then weight predictions  
 172 from each model equally, using them to predict a mean  
 173 initial beam density distribution Fig. 2(a-e) with asso-  
 174 ciated confidence intervals Fig. 2(f-j). Performing this  
 175 analysis by tracking  $10^5$  particles for each image took  
 176 less than 30 seconds per ensemble sample using a profes-  
 177 sional grade GPU ( $< 60$  ms per iteration, 500 steps per  
 178 ensemble sample).

TABLE I. Predicted Emittances Compared to True Values

Parameter	Ground truth	RMS Prediction	Reconstruction	Unit
$\varepsilon_x$	2.00	2.47	$2.00 \pm 0.01$	mm-mrad
$\varepsilon_y$	11.45	14.10	$10.84 \pm 0.04$	mm-mrad
$\varepsilon_{4D}$	18.51	34.83*	$17.34 \pm 0.08$	mm <sup>2</sup> -mrad <sup>2</sup>

\* Assumes x-y phase space independence

179 We see excellent agreement between the average recon-  
 180 structed and synthetic projections in both transverse cor-  
 181 related and uncorrelated phase spaces. Furthermore, the  
 182 prediction uncertainty from ensembling is on the order of  
 183 a few percent relative to the predicted mean, providing  
 184 confidence that the overall solution found during opti-  
 185 mization is unique. As shown in Table I, reconstructions  
 186 of the beam distribution from image data predicts trans-  
 187 verse phase space emittances that are closer to ground  
 188 truth values than those predicted from second-order mo-  
 189 ment measurements of the transverse beam distribution.

190 This results from non-linearities and cross-correlations  
191 present in the 4-D transverse phase space distribution.

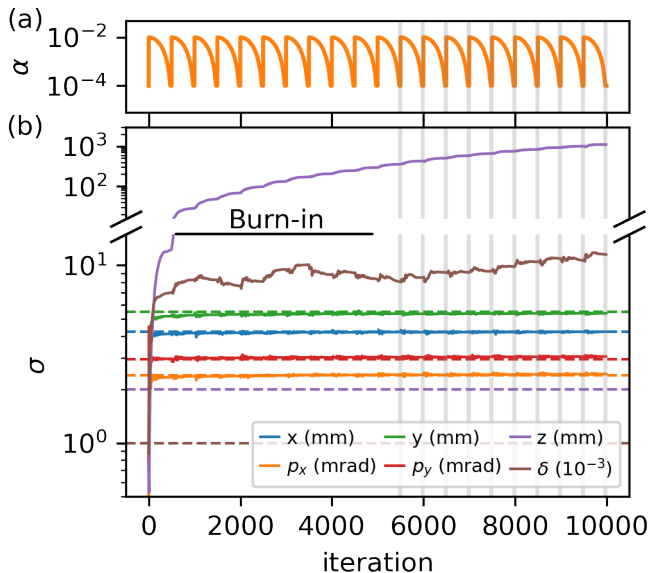


FIG. 3. Evolution of the proposal distribution during training on synthetic data. (a) Learning rate schedule for snapshot ensembling. (b) Second order moments of beam reconstruction during training for each phase space coordinate. Dashed lines denote ground truth values. Vertical lines denote snapshot locations after burn-in period.

192 It is instructive to examine the evolution of the pro-  
193 posal distribution during model training. In Fig. 3(b)  
194 we examine second order scalar metrics of the proposal  
195 distribution after each training iteration for each phase  
196 space coordinate. The entropy term in Eq. 1 causes  
197 the distribution to expand in 6D phase space until con-  
198 strained by experimental evidence. Phase space com-  
199 ponents that have the strongest impact on beam trans-  
200 port through the beamline as a function of quadrupole  
201 strength converge quickly to the true values, whereas  
202 the ones that have little-to-no impact (e.g. the longi-  
203 tudinal distribution characteristics) continue to grow. In  
204 other cases, there is weak coupling between the experi-  
205 mental measurements and beam properties; for example,  
206 chromatic focusing effects due to the energy spread  $\sigma_\delta$   
207 of the beam weakly affect the measured images. Here,  
208 the reconstruction can only provide an upper-bound es-  
209 timate of the energy spread, since small changes in trans-  
210 verse beam propagation due to chromatic aberrations are  
211 overshadowed by statistically dominated particle motion.  
212 Convergence of the proposal distribution thus provides a  
213 useful indicator of which phase space components can  
214 be reliably reconstructed from arbitrary sets of measure-  
215 ments.

216 We now describe a demonstration of our method on  
217 an experimental example at the Argonne Wakefield Ac-  
218 celerator (AWA) [35] facility at Argonne National Labo-  
219 ratory. Our objective is to identify the phase space dis-

220 tribution of 65-MeV electron beams at the end of the  
221 primary accelerator beamline. The focusing strength  
222 of a quadrupole, with an effective length of 12 cm, is  
223 scanned while imaging the beam at a transverse scintillat-  
224 ing screen located 3.38 m downstream. Charge window-  
225 ing, image filtering, thresholding and downsampling were  
226 used to generate a set of 3 images for each quadrupole  
227 setting (see the Supplemental Materials for additional  
228 details).

TABLE II. Predicted Emittances from Experimental Data

Parameter	RMS Prediction	Reconstruction	Unit
$\varepsilon_{x,n}$	$4.18 \pm 0.71$	$4.23 \pm 0.02$	mm-mrad
$\varepsilon_{y,n}$	$3.65 \pm 0.36$	$3.42 \pm 0.02$	mm-mrad

229 We developed a differentiable simulation in Bmad-X of  
230 the experimental beamline, including details of the diag-  
231 nostics used, such as the location and properties of beam-  
232 line elements and the per-pixel resolution of the imaging  
233 screen. With this simulation, we used our method to  
234 reconstruct the beam distribution from experimentally-  
235 measured transverse beam images. The results, as shown  
236 in Figure 4 and Table II, demonstrate good agreement  
237 between experimental measurements of the beam distri-  
238 bution and predictions from our reconstruction. Scalar  
239 predictions of the beam emittances from the image-based  
240 reconstruction are consistent with those calculated from  
241 RMS measurements. Additionally, our reconstruction  
242 method accurately reproduces fine features of the trans-  
243 verse beam distribution that were not present in the  
244 training data set.

245 In this work, we have demonstrated how differentiable  
246 particle tracking simulations, combined with neural net-  
247 work based representations of beam distributions, can be  
248 used to interpret common image-based diagnostic mea-  
249 surements. Our method produces detailed reconstruc-  
250 tions of 4-dimensional transverse phase space distribu-  
251 tions from limited data sets, without the use of com-  
252 plex phase space manipulations or specialized diagnos-  
253 tics. Additionally, our reconstruction identifies limita-  
254 tions in resolving certain aspects of the beam distribu-  
255 tion based on available measurements. This analysis is  
256 enabled by inexpensive gradient calculations provided by  
257 backwards differentiable physics simulations. As a result,  
258 we are able to determine thousands of free parameters  
259 used to describe complex beam distributions on a time  
260 scale similar to the time it takes to perform the physical  
261 tomographic measurements themselves. Thus, our recon-  
262 struction technique is suitable for inferring detailed beam  
263 distributions in an online fashion, i.e. during accelerator  
264 operations.

265 As with any new algorithmic technique, there are areas  
266 for future improvement. Uncertainty estimates provided  
267 by the reconstruction algorithm only capture systematic

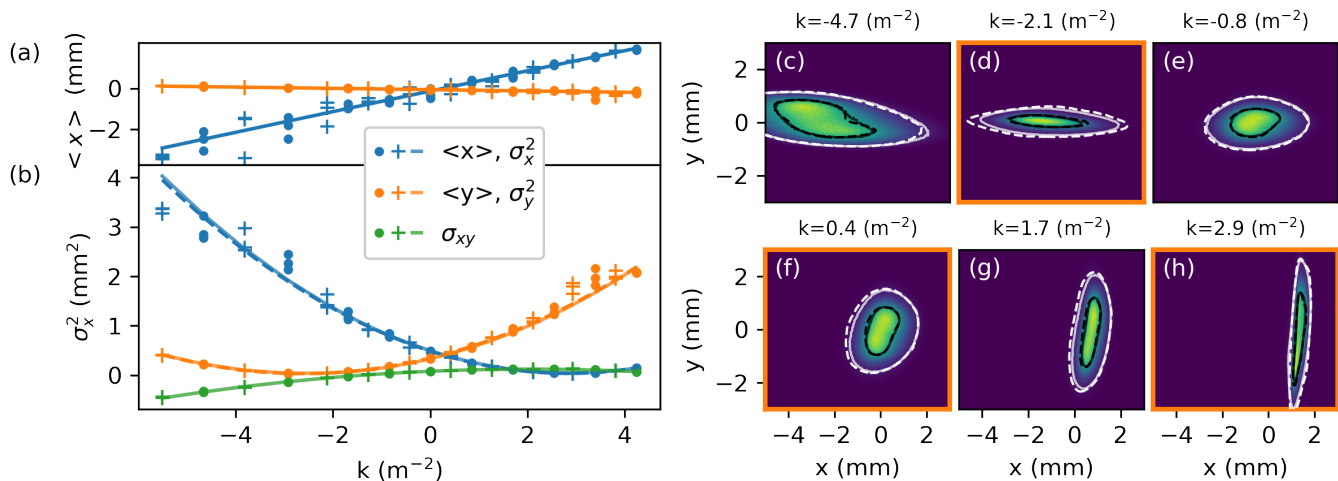


FIG. 4. Reconstruction results from experimental measurements at AWA. Comparison between measured and predicted beam centroids (a) and second-order beam moments (b) on the diagnostic screen as a function of geometric quadrupole focusing strength ( $k$ ). Points denote training samples and crosses denote test samples. Dashed line shows second order polynomial fit of training data and solid line shows predictions from image-based phase space reconstruction. We also compare (c-h) screen images and reconstructed predictions for a subset of quadrupole strengths. Contours denote the 50<sup>th</sup> (black) and 95<sup>th</sup> (white) percentiles of the measured (dashed) and predicted (solid) screen distributions. Orange borders denote test samples.

268 uncertainties from optimizing the loss function, Eq. 1; thus it ignores systematic uncertainties of the physical  
 269 measurement and stochastic noise inherent in real ac-  
 270 celerators. Future work will incorporate Bayesian anal-  
 271 ysis techniques into the reconstruction to provide cali-  
 272 brated uncertainty estimates to experimental measure-  
 273 ments. Also, while our method significantly increases the  
 274 speed of high-dimensional phase space reconstructions,  
 275 achieving this requires substantial amounts of memory  
 276 to store the derivative information of each macro-particle  
 277 at every tracking step ( $\sim 4$  GB for each snapshot in the  
 278 analysis performed here). Peak memory consumption  
 279 can be reduced through the use of checkpointing [36] or  
 280 pre-computing derivatives associated with tracking parti-  
 281 cles through the entire beamline. Finally, this method  
 282 is limited by the availability of accurate, computationally  
 283 efficient, backwards differentiable particle tracking  
 284 simulations. In order to expand the range of diagnostic  
 285 measurements that can be analyzed by this technique,  
 286 further investment in differentiable implementations of  
 287 particle tracking simulations is needed.

289 This new reconstruction approach opens the door to ef-  
 290 ficient, detailed characterization of 6-dimensional phase  
 291 space distributions and new types of compound diag-  
 292 nostic measurements. By adding longitudinal beam ma-  
 293 nipulations, such as transverse deflecting cavities paired  
 294 with dipole spectrometers, to the beamline used here, full  
 295 phase space distributions can be characterized through a  
 296 series of quadrupole strength and deflecting cavity phase  
 297 scans.

298 The authors would like to thank Lukas Heinrich and  
 299 Michael Kagan for useful discussion during the early con-

300 ceptual development of this work. This work was sup-  
 301 ported by the U.S. Department of Energy, under DOE  
 302 Contract No. DE-AC02-76SF00515, the Office of Sci-  
 303 ence, Office of Basic Energy Sciences and the Center  
 304 for Bright Beams, NSF award PHY-1549132. This re-  
 305 search used resources of the National Energy Research  
 306 Scientific Computing Center (NERSC), a U.S. Depart-  
 307 ment of Energy Office of Science User Facility located  
 308 at Lawrence Berkeley National Laboratory, operated un-  
 309 der Contract No. DE-AC02-05CH11231 using NERSC  
 310 award ERCAP0020725.

311 Author Contributions: R.R. and A.E. conceived of the  
 312 idea to combine differentiable simulations with machine  
 313 learning for phase space tomography. R.R. led the studies  
 314 and performed the work for phase space reconstruction.  
 315 A.E. and D.R. provided technical guidance and feedback.  
 316 J.P.G. developed the differentiable simulation with guid-  
 317 ance from R.R. and C.M.. S.K., E.W. and J.P. assisted  
 318 with experimental studies at AWA. R.R. and A.E. wrote  
 319 the manuscript. J.P.G., C.M. provided substantial edits  
 320 to the manuscript. All authors provided feedback on the  
 321 manuscript.

\* rroussel@slac.stanford.edu

[1] S. Nagaitsev, Z. Huang, J. Power, J. L. Vay, P. Piot, L. Spentzouris, J. Rosenzweig, Y. Cai, S. Cousineau, M. Conde, M. Hogan, A. Valishev, M. Minty, T. Zolkin, X. Huang, V. Shiltsev, J. Seeman, J. Byrd, Y. Hao, B. Dunham, B. Carlsten, A. Seryi, and R. Patterson, Accelerator and beam physics research goals and oppor-

- tunities (2021).
- [2] P. Emma, R. Akre, J. Arthur, R. Bionta, C. Bostedt, J. Bozek, A. Brachmann, P. Bucksbaum, R. Coffee, F. J. Decker, Y. Ding, D. Dowell, S. Edstrom, A. Fisher, J. Frisch, S. Gilevich, J. Hastings, G. Hays, P. Hering, Z. Huang, R. Iverson, H. Loos, M. Messerschmidt, A. Miahnahri, S. Moeller, H. D. Nuhn, G. Pile, D. Ratner, J. Rzepiela, D. Schultz, T. Smith, P. Stefan, H. Tompkins, J. Turner, J. Welch, W. White, J. Wu, G. Yocky, and J. Galayda, First lasing and operation of an aangstrom-wavelength free-electron laser, *Nature Photonics* **4**, 641 (2010), publisher: Nature Publishing Group.
- [3] H. Li, Y. Sun, J. Vila-Comamala, T. Sato, S. Song, P. Sun, M. H. Seaberg, N. Wang, J. B. Hastings, M. Dunne, P. Fuoss, C. David, M. Sutton, and D. Zhu, Generation of highly mutually coherent hard-x-ray pulse pairs with an amplitude-splitting delay line, *Phys. Rev. Research* **3**, 043050 (2021).
- [4] Y. Sun, M. Dunne, P. Fuoss, A. Robert, D. Zhu, T. Osaka, M. Yabashi, and M. Sutton, Realizing split-pulse x-ray photon correlation spectroscopy to measure ultrafast dynamics in complex matter, *Phys. Rev. Research* **2**, 023099 (2020).
- [5] A. Marinelli, D. Ratner, A. A. Lutman, J. Turner, J. Welch, F. J. Decker, H. Loos, C. Behrens, S. Gilevich, A. A. Miahnahri, S. Vetter, T. J. Maxwell, Y. Ding, R. Coffee, S. Wakatsuki, and Z. Huang, High-intensity double-pulse x-ray free-electron laser, *Nature Communications* **6**, 10.1038/ncomms7369 (2015).
- [6] F.-J. Decker, K. L. Bane, W. Colocho, S. Gilevich, A. Marinelli, J. C. Sheppard, J. L. Turner, J. J. Turner, S. L. Vetter, A. Halavanau, C. Pellegrini, and A. A. Lutman, Tunable x-ray free electron laser multipulses with nanosecond separation, *Scientific Reports* **12**, 10.1038/s41598-022-06754-y (2022).
- [7] *Advanced Accelerator Development Strategy Report: DOE Advanced Accelerator Concepts Research Roadmap Workshop*, Tech. Rep. (USDOE Office of Science, Washington, DC (United States), 2016).
- [8] G. Ha, K.-J. Kim, J. Power, Y. Sun, P. Piot, *et al.*, Bunch shaping in electron linear accelerators, *Reviews of Modern Physics* **94**, 025006 (2022).
- [9] C. McKee, P. O’Shea, and J. Madey, Phase space tomography of relativistic electron beams, *Nuclear Instruments and Methods in Physics Research Section A: Accelerators, Spectrometers, Detectors and Associated Equipment* **358**, 264 (1995).
- [10] S. Hancock, M. Lindroos, E. McIntosh, and M. Metcalf, Tomographic measurements of longitudinal phase space density, *Computer Physics Communications* **118**, 61 (1999).
- [11] D. Stratakis, R. A. Kishek, I. Haber, M. Walter, R. B. Fiorito, S. Bernal, J. Thangaraj, K. Tian, C. Papadopoulos, M. Reiser, and P. G. O’Shea, Phase space tomography of beams with extreme space charge, in *2007 IEEE Particle Accelerator Conference (PAC)* (2007) pp. 2025–2029.
- [12] V. Yakimenko, M. Babzien, I. Ben-Zvi, R. Malone, and X.-J. Wang, Electron beam phase-space measurement using a high-precision tomography technique, *Physical Review Special Topics - Accelerators and Beams* **6**, 122801 (2003).
- [13] M. Röhrs, C. Gerth, H. Schlarb, B. Schmidt, and P. Schmüser, Time-resolved electron beam phase space tomography at a soft x-ray free-electron laser, *Physical Review Special Topics - Accelerators and Beams* **12**, 050704 (2009).
- [14] M. Gordon, W. Li, M. Andorf, A. Bartnik, C. Duncan, M. Kaemingk, C. Pennington, I. Bazarov, Y.-K. Kim, and J. Maxson, Four-dimensional emittance measurements of ultrafast electron diffraction optics corrected up to sextupole order, *Physical Review Accelerators and Beams* **25**, 084001 (2022).
- [15] A. Green and Y.-M. Shin, Implementation of Quadrupole-scan Emittance Measurement at Fermilab’s Advanced Superconducting Test Accelerator (ASTA), in *6th International Particle Accelerator Conference* (2015) p. MOPMA052.
- [16] E. Prat and M. Aiba, Four-dimensional transverse beam matrix measurement using the multiple-quadrupole scan technique, *Physical Review Special Topics - Accelerators and Beams* **17**, 052801 (2014).
- [17] A. Mostacci, M. Bellaveglia, E. Chiadroni, A. Cianchi, M. Ferrario, D. Filippetto, G. Gatti, and C. Ronsivalle, Chromatic effects in quadrupole scan emittance measurements, *Phys. Rev. ST Accel. Beams* **15**, 082802 (2012).
- [18] S. Webb, *The Physics of Medical Imaging* (CRC Press, Boca Raton, 1987).
- [19] A. C. Kak and M. Slaney, *Principles of computerized tomographic imaging* (SIAM, 2001).
- [20] A. Wolski, D. Christie, B. Militsyn, D. Scott, and H. Kockelbergh, Transverse phase space characterization in an accelerator test facility, *Physical Review Accelerators and Beams* **23**, 032804 (2020).
- [21] A. Wolski, M. A. Johnson, M. King, B. L. Militsyn, and P. H. Williams, Transverse phase space tomography in the clara accelerator test facility using image compression and machine learning, arXiv preprint arXiv:2209.00814 (2022).
- [22] K. M. Hock and M. G. Ibson, A study of the maximum entropy technique for phase space tomography, *Journal of Instrumentation* **8** (02), P02003.
- [23] K. Hock and A. Wolski, Tomographic reconstruction of the full 4d transverse phase space, *Nuclear Instruments and Methods in Physics Research Section A: Accelerators, Spectrometers, Detectors and Associated Equipment* **726**, 8 (2013).
- [24] J. C. Wong, A. Shishlo, A. Aleksandrov, Y. Liu, and C. Long, 4D transverse phase space tomography of an operational hydrogen ion beam via noninvasive 2D measurements using laser wires, *Physical Review Accelerators and Beams* **25**, 042801 (2022).
- [25] A. Scheinker, Adaptive Machine Learning for Robust Diagnostics and Control of Time-Varying Particle Accelerator Components and Beams, *Information* **12**, 161 (2021), number: 4 Publisher: Multidisciplinary Digital Publishing Institute.
- [26] M. Wang, Z. Wang, D. Wang, W. Liu, B. Wang, M. Wang, M. Qiu, X. Guan, X. Wang, W. Huang, and S. Zheng, Four-dimensional phase space measurement using multiple two-dimensional profiles, *Nuclear Instruments and Methods in Physics Research Section A: Accelerators, Spectrometers, Detectors and Associated Equipment* **943**, 162438 (2019).
- [27] B. Hermann, V. A. Guzenko, O. R. Hürzeler, A. Kirchner, G. L. Orlandi, E. Prat, and R. Ischebeck, Electron beam transverse phase space tomography using

- nanofabricated wire scanners with submicrometer resolution, *Physical Review Accelerators and Beams* **24**, 022802 (2021).
- [28] D. Sagan, Bmad: A relativistic charged particle simulation library, *Computational accelerator physics. Proceedings, 8th International Conference, ICAP 2004, St. Petersburg, Russia, June 29-July 2, 2004*, Nucl. Instrum. Meth. **A558**, 356 (2006), proceedings of the 8th International Computational Accelerator Physics Conference.
- [29] J. Lawson, R. Gluckstern, and P. M. Lapostolle, Emission, entropy and information, Part. Accel. **5**, 61 (1973).
- [30] D. P. Kingma and J. Ba, Adam: A Method for Stochastic Optimization, arXiv:1412.6980 [cs] (2017), arXiv:1412.6980.
- [31] Y. A. LeCun, L. Bottou, G. B. Orr, and K.-R. Müller, Efficient BackProp, in *Neural Networks: Tricks of the Trade: Second Edition*, Lecture Notes in Computer Science, edited by G. Montavon, G. B. Orr, and K.-R. Müller (Springer, Berlin, Heidelberg, 2012) pp. 9–48.
- [32] A. Paszke, S. Gross, F. Massa, A. Lerer, J. Bradbury, G. Chanan, T. Killeen, Z. Lin, N. Gimelshein, L. Antiga, A. Desmaison, A. Kopf, E. Yang, Z. DeVito, M. Raieson, A. Tejani, S. Chilamkurthy, B. Steiner, L. Fang, J. Bai, and S. Chintala, PyTorch: An Imperative Style, High-Performance Deep Learning Library, in *Advances in Neural Information Processing Systems 32*, edited by H. Wallach, H. Larochelle, A. Beygelzimer, F. d. Alché-Buc, E. Fox, and R. Garnett (Curran Associates, Inc., 2019) pp. 8024–8035.
- [33] M. Rosenblatt, Remarks on some nonparametric estimates of a density function, *The annals of mathematical statistics* , 832 (1956).
- [34] G. Huang, Y. Li, G. Pleiss, Z. Liu, J. E. Hopcroft, and K. Q. Weinberger, Snapshot ensembles: Train 1, get m for free, arXiv preprint arXiv:1704.00109 (2017).
- [35] M. Conde, S. Antipov, D. Doran, W. Gai, Q. Gao, G. Ha, C. Jing, W. Liu, N. Neveu, J. Power, *et al.*, Research program and recent results at the argonne wakefield accelerator facility (awa), Proc. IPAC'17 , 2885 (2017).
- [36] B. Dauvergne and L. Hascoët, The data-flow equations of checkpointing in reverse automatic differentiation, in *International Conference on Computational Science* (Springer, 2006) pp. 566–573.